



Study on the Performance of Ball Mill with Liner Structure based on DEM

Zhanfu Li¹, Yaokun Wang², Kunyuan Li¹, Wenyu Lin¹ & Xin Tong^{1*}

¹School of Mechanical and Automobile Engineering, Fujian University of Technology, Fuzhou, Fujian, 350118, China.

²School of Mechanical Engineering and Automation, Huaqiao University, Xiamen 361021, China

*E-mail: Tongxin_hqu_fjut@163.com

Abstract. This study used the discrete element method (DEM), which is effective and popular for solving the problem of granular systems simulating the motion of particles in a ball mill in different structural forms and at different rotational speeds. Firstly, simulations of five kinds of lifters (triangular, trapezoidal, rectangular, ladder and hemispherical) were set up. The results were as follows: when the rectangular lifter was selected as mill liner, the ball mill efficiency was significantly high. The breaking performance of the hemispherical lifter and the ladder lifter was poor, because the main pattern of motion was grinding rather than impact breakage. Secondly, the effects of the height-width ratio of the rectangular lifter, the height of the lifter and the number of lifters on the working efficiency of the ball mill were studied. It was found that a number of rectangular lifters of 12 and a height-width ratio of 3:1 produced the best results. The best height of the rectangular lifter was about 13 mm. Lastly, displacement, stress and deformation were analyzed using DEM coupled with a finite element method (FEM). The purpose was to design the geometrical lifter structure and to improve the performance of the ball mill.

Keywords: ball mill; DEM; height-width ratio; rectangular lifter; number of lifter.

1 Introduction

Ball mills, which crush and grind ore or other materials, are widely used in bio-pharmaceutical, construction and other industries. There are several advantages to using this equipment, such as the high breakage rate, the broad range of materials that can be processed, its simple structure in view of maintenance, and good adaption to bad environments over a long period of time [1-4]. Based on these advantages, a great deal of fundamental industries use this equipment to grind raw materials. Hence, it is significant and valuable to do an in-depth study on this subject.

When a ball mill rotates, the ore and media are subjected to gravity, centrifugal force and friction, and at the same time are raised by the liners and lifters. When

Received October 16th, 2017, Revised March 21st, 2017, Accepted for publication April 5th, 2018.

Copyright ©2018 Published by ITB Journal Publisher, ISSN: 2337-5779, DOI: 10.5614/j.eng.technol.sci.2018.50.2.2

the mill rotates at a certain angle, the gravity exceeds the centrifugal force. Then the ore and media will fall and collide or grind. Eventually, the ore will be small enough as a result of this colliding and grinding. It is extremely difficult to investigate the motion of the media inside a mill, because the motions of particles are always random, complicated and discrete. When the discrete element method (DEM) – which is very powerful in studying the kinetics of discrete elements – was introduced, it provided a new solution for simulating the motion of media in a ball mill [5-9]. Recently, several researchers have investigated the parameters of structure and movement and got many valuable results using DEM. Djordjevic studied the influence of liner height, number of bars and the friction coefficient between the liner and the medium on grinding efficiency [10-11]. Operation conditions, including rotation speed, number of grinding balls and material in collision, were studied by DEM in terms of energy in Ref. [12]. A performance evaluation was conducted on the breakage process in a ball mill along with DEM modeling in Ref. [13]. Using a representative non-round ore, simulation of particle breakage was conducted to study different concave profiles and mantles with DEM in Ref. [8]. DEM simulations were proven to be an effective way to solve ball mill problems in Ref. [14]. Meanwhile, Ping Yu and Powell, *et al.* used equations to describe the dynamic condition of a tumbling mill [15]. The accumulation of harder (tougher) components in a mill as the grinding progresses has been analyzed by Tavares [16]. The effective power and specific power definitions are too complex to calculate. In this paper, we introduce a new index to assess ball mill performance by combining the reduction of kinetic energy with the number of collisions.

Numerical modeling with DEM in particle motion and breakage are important for improved operation of mills and vibrating screens [17-21]. In recent years, in order to deeply understand the wear and stress state, a combined DEM and finite element method has been developed to solve these. Wang, *et al.* studied friction behavior by coupling DEM with a finite element method (FEM) [22]. Murugaratnam, *et al.* used this method to optimize the shot peening process [23]. Xia, *et al.* analyzed the stress distribution on the screen surface with DEM-FEM [24]. P. Jonsén designed the mill liner structure with DEM-FEM [25]. In this paper, DEM-FEM was used to calculate total deformation, equivalent stress and strain energy of mill lifters.

2 Discrete Element Method and Simulations

DEM was proposed by Cundall and Strack in 1979. It is a special class of numerical schemes for simulating the behavior of discrete interacting particles [26]. In this method, every separate particle is regarded as an independent body. There are only two conditions of these bodies, contact and separation. Once

there is contact between two discs, the normal and shear forces can be solved by the equation of the force-displacement law. When the contact forces are clear, the new displacement can be calculated using Newton's second law and the central difference method. Because this procedure is carried out for every disc in the system, the disc's positions at the next instant of time is gotten. A flow diagram of the mutual contact particle unit cycle is shown below (Figure 1).

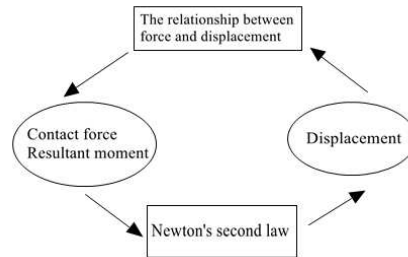


Figure 1 Calculation schematic of contact particle.

2.1 Force-Displacement Equation

When the two particle units are in contact with each other, a certain amount of relative sliding displacement is generated. The force obtained by the contact between the particle units can be solved by the force-displacement equation according to the relative sliding displacement. First, the contact force between the particle unit and the relative sliding displacement are divided into tangential and normal parts. The normal force of the two particles at the point of contact is F_n , the relative slip displacement between the particle units is u_n , and the normal contact stiffness is k_n . Thus, the normal force-displacement equation of the two particle units based on the following equation:

$$F_n = k_n u_n \tag{1}$$

The shear force between the particles in the tangential direction is described by incremental means. Assuming that the tangential shear force of the particles is F_s , the tangential relative slip displacement between the particle units is u_s , and the tangential contact stiffness is k_s , the tangential force-displacement equation of two particle units based on the following equation:

$$\Delta F_s = k_s \Delta u_s \tag{2}$$

2.2 Discrete Element Motion Equation

The motion of the macroscopic discrete system can be obtained by accumulating the amount of displacement and the contact force at each time

step. The basic solution to the idea is through the force-displacement equation, as long as the amount of displacement can be determined to solve the particle unit by the force. The displacement can be calculated using Newton's second law. With Newton's second law it is easy to solve the motion equation of particle i , as follows:

$$\left. \begin{aligned} m_i u_i'' &= \sum F \\ I_i \theta_i'' &= \sum M \end{aligned} \right\} \quad (3)$$

In the above formula, θ_i'' and u_i'' denote the angular acceleration and the acceleration of the i -th particle. $\sum M$ and $\sum F$ denote the combined force and the combined torque of the i -th particle. I_i and m_i represent the moment of inertia and the mass of the i -th particle. By using the central difference method for Eqs. (1) to (3) respectively to calculate the numerical integration, the update speed is the intermediate point of two iterative time steps and can be expressed as follows:

$$\left. \begin{aligned} (u_i')_{N+\frac{1}{2}} &= (u_i')_{N-\frac{1}{2}} + [\sum F / m_i]_N \Delta t \\ (\theta_i')_{N+\frac{1}{2}} &= (\theta_i')_{N-\frac{1}{2}} + [\sum M / I_i]_N \Delta t \end{aligned} \right\} \quad (4)$$

where Δt is the time step and N represents the corresponding time point. The corresponding displacement and angle expressions can be obtained in Eq. (5) by integrating Eqs. (1) to (4) as follows:

$$\left. \begin{aligned} (u_i)_{N+1} &= (u_i)_N + (u_i')_{N+\frac{1}{2}} \Delta t \\ (\theta_i)_{N+1} &= (\theta_i)_N + (\theta_i')_{N+\frac{1}{2}} \Delta t \end{aligned} \right\} \quad (5)$$

2.3 Ball Mill Model

The main structure of the ball mill is composed of three parts, namely the feed inlet, the cylinder part (work bin), and the discharge port. Figure 2(a) shows the structural model of a ball mill. In the mill cylinder part, there are lifters for turning over the particles. The quartz sand particles enter the cylinder through a feed screw structure in the feed port. They collide and are ground between the various particles in the cylinder to achieve the target grain size. Then the particles pass through a grate plate hole into the discharge port and the milling process is completed.

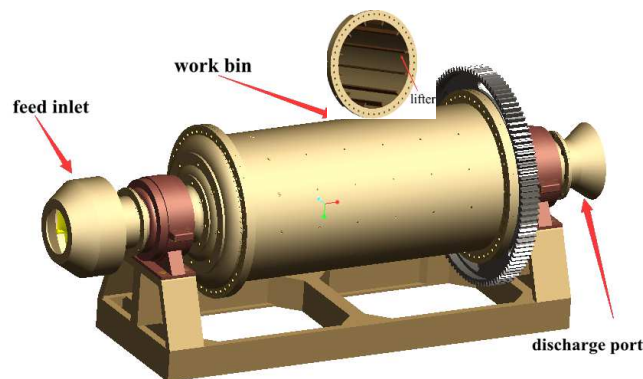


Figure 2 3D-model of a ball mill.

Considering the structural parameters of the ball mill and the time of simulation it is not necessary to use the whole model in the simulation. Figure 3 shows the internal structure of the ball mill cylinder model. To do the corresponding simplified calculations, only the main structure of the ball mill cylinder has to be expressed. This reduces simulation time and improves the efficiency of the simulation calculations.

3 Simulation and Analysis

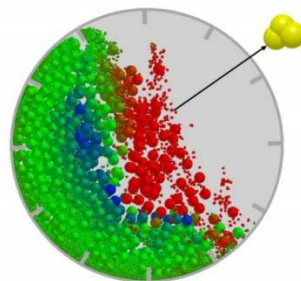


Figure 3 Simulation of grinding and particle model.

The ore model in the ball mill movement simulation was created by using a multi-sphere approach. A plurality of smaller balls can be stacked so that the envelopes formed by them are close to the actual ore profile. This combination was used as the simulated ore model. The study object were quartz sand particles with a size of about 6 mm. The shape of the medium was spherical, with a diameter of 10 mm. The diagrams of ore and steel balls are shown in the Figure 3. In this paper, a specific $\phi 900mm \times 1800mm$ ball mill was selected. Since

the particles in the cylinder are distributed evenly in the axial direction, the movement of the particles in the axial direction can be neglected. In order to shorten the simulation time and improve calculation efficiency, the simulation experiment was carried out on a section of the cylinder in the axial direction. Therefore, the length of the cylinder model in the experiment was 25.5 mm. Meanwhile, the diameter of the medium was 10 mm and the number of particles was set to 100. Experiments were carried out to simulate quartz sand particles with a particle size of about 6 mm and the number of quartz particles was set to 1000. The parameters are shown in Table 1.

Table 1 Simulation parameters.

	Steel ball	Quartz sand	Liner
Poisson's ratio	0.3	0.3	0.3
Shear modulus (Pa)	7e+10Pa	1e+07Pa	7e+10Pa
Density (kg/m ³)	7800	1600	7800
Coefficient of restitution	0.5	0.2	0.5
Static friction coefficient	0.5	0.5	0.5
Rolling friction coefficient	0.01	0.01	0.01

3.1 Milling Rate and Data Analysis

The steel balls are lifted to a certain height by the lifters and the centrifugal force. When the gravity exceeds the centrifugal force, the steel balls follow a cascading motion where the balls flow down the free surface of the charge or a cataracting motion where the balls are thrown away from the surface and follow a parabolic path [2]. When the steel balls and ore particles collide or grind, the collision or grinding consumes kinetic energy. The amount of change in kinetic energy is defined in Eq. (6) as follows:

$$\Delta E_k = \Delta E_k^+ + \Delta E_k^- \quad (6)$$

where ΔE_k , ΔE_k^+ , ΔE_k^- are the change of overall kinetic energy, the increment of kinetic energy and the decrement of kinetic energy of the whole system of particles, respectively. The overall kinetic energy increment of the particles is derived from the external energy supply and the conversion of the potential energy. In the stable operation stage, the power of the ball mill and the total potential energy of the particles are constant. The total kinetic energy increment of the particles is similar to ($\Delta E_k^+ = const$). The total kinetic energy reduction of the particles is equal to the energy consumed in collision and friction, i.e. the kinetic energy reduction of the particles is a variable and only related to collision (W_c) and friction work (W_f) in the following Eq. (7):

$$\Delta E_k^- = W_c + W_f \quad (7)$$

Therefore, the first-order change of kinetic energy is a variable about the external energy supply, the conversion of potential energy, collision and friction, and the second-order change of kinetic energy is only about the collision and friction variables in the following Eq. (8):

$$\Delta(\Delta E_k) = \Delta(\Delta E_k^-) = \Delta(W_c + W_f) \tag{8}$$

where $\Delta(\Delta E_k)$, $\Delta(\Delta E_k^-)$ represents the second-order change of the total kinetic energy and the second-order reduction of the total kinetic energy of the particles. In this paper, we selected milling rate η , which is the ratio of the second-order change of kinetic energy and the number of all contacts between the particles. In other words, the milling rate indicates the consumption of kinetic energy in a single contact to characterize the working performance of the ball mill. A greater milling rate means greater kinetic energy consumption in a single contact, which means better breakage in the following Eq. (9):

$$\eta = \frac{\Delta(\Delta E_k)}{N} \tag{9}$$

where $\Delta(\Delta E_k)$ represents the second-order change of the total kinetic energy of the particles and N is the number of contacts between all particles at that moment.

3.2 Influence of Lifter Profile

Table 2 Parameter settings of lifter profile.

Lifter shape	Rotation speed (rad/min)	Number of lifters	Height of lifters (mm)	Simulation time (s)
Rectangle	5	12	12	10
Trapezoid				
Triangle				
Ladder				
Semicircle				

The lifters not only play an important role in protecting the cylinder but also raise the media to a high place to achieve crushing. The profile of the lifters affects the media's trajectory and height, which also affects the efficiency of the ball mill. Therefore, the effect of different lifter profiles on the motion of the media was analyzed in a simulation experiment. An appropriate lifter profile can significantly improve the working efficiency of the ball mill. In these simulations, five profiles (rectangular, trapezoidal, triangular, ladder, and semicircle) were used to analyze their influence. The simulation parameters are shown in Table 2.

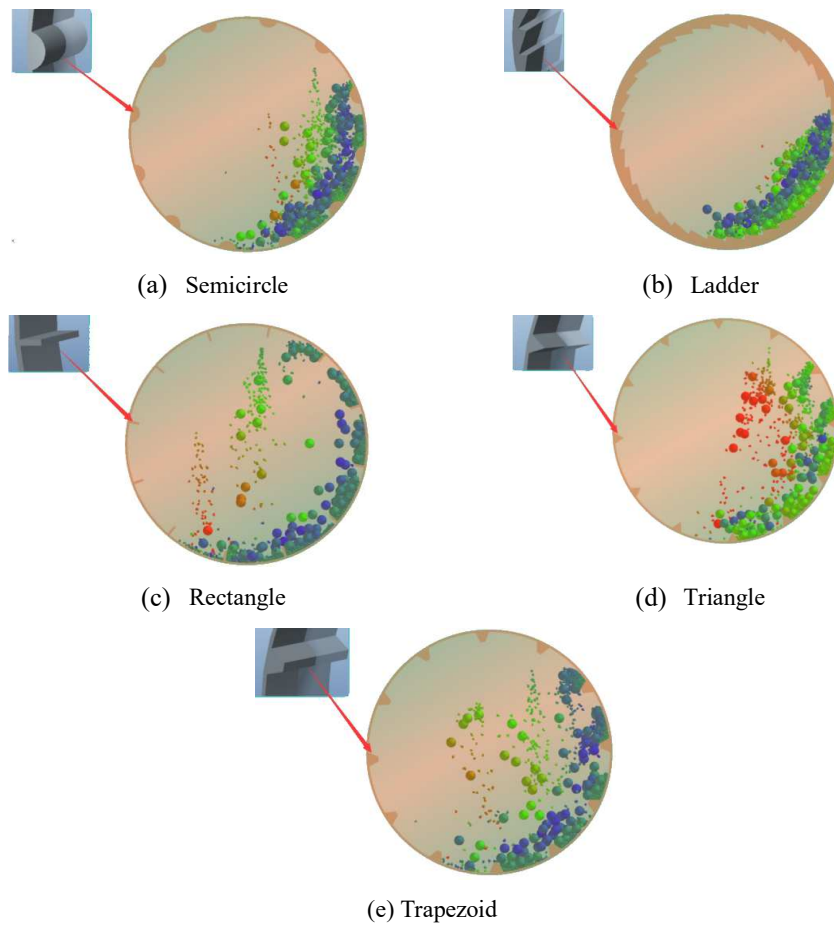


Figure 4 (a), (b), (c), (d), and (e) display the different lifter profiles used in the simulations.

The trajectories of the media for different lifter profiles are shown in Figure 4. It can be seen that the lifting effects of the rectangular lifter, the trapezoidal lifter and the triangular lifter on the media were better than those of the ladder and semicircular lifters, and it was more favorable for the particles to follow a cataracting motion, where the balls are thrown away from the surface and follow a parabolic path. The lifting height of the rectangular lifter was the highest and the crushing effect was also the best for this lifter. Because the lifting heights of the ladder lifter and the semicircular lifter were low, the particles mainly flowed down the free surface of the charge and the breakage effect was poor.

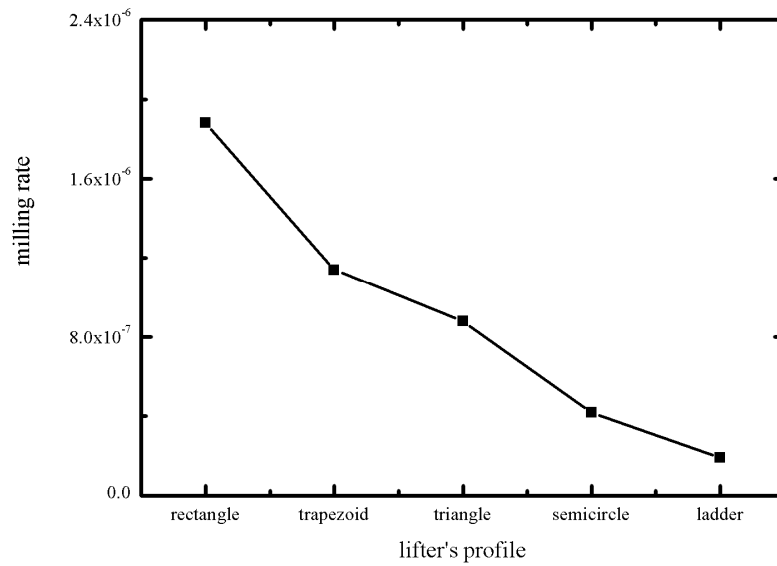


Figure 5 Relationship between milling rate and lifter's profile.

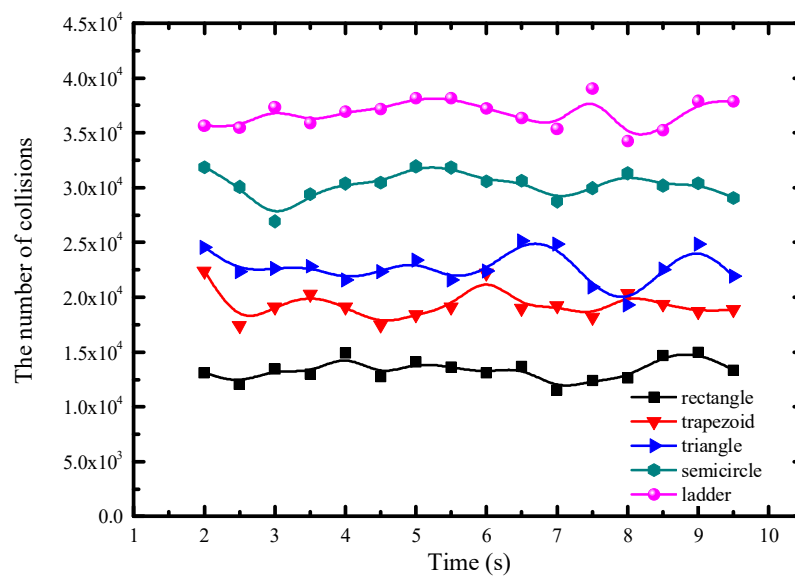


Figure 6 Number of collisions for different lifters.

Observing the process in the experiments, the stable stage was selected for analysis. Comparing Figures 5 with 6, it can be seen that the numbers of

collisions between all the particles for the rectangular lifter, the triangular lifter, and the trapezoidal lifter were smaller than those of the ladder lifter and the semicircle lifter, but their milling rates were higher. The experiment that used rectangular lifters had the least amount of collisions between all the particles, while it had the highest milling rate compared to the others. It also shows that in the experiment with rectangular lifters, there were more effective collisions than in the other experiments. The number of collisions between all particles for the ladder lifters was the highest, but the milling rate was the lowest. This also shows that a ball mill with ladder lifters mostly does ineffective work, which not only cannot effectively improve ball mill production efficiency but also increases the energy consumption of the equipment.

3.3 Influence of Rectangular Lifter's Height-Width Ratio

The height-width ratio of a rectangular lifter is the ratio of the height to the thickness of the lifter. A change in the height-width ratio of the rectangular lifter directly affects the thickness of the lifters and the weight of the lifters. If the lifters are too heavy, much of energy used for making the cylinder rotate is wasted. Therefore, choosing the appropriate height-width ratio can maximize the effective power of the ball mill and reduce energy loss. In the study of the height-width ratio of rectangular lifter, five sets of experiments were conducted with height-width ratios set to 5:1, 3:1, 1:1, 1:3, 1:5, respectively, and the height of the lifters at 12 mm. The experimental scheme is shown in Table 3. The simulations with different height-width ratios are presented in Figure 7.

Table 3 Parameter settings of lifter height-width ratio.

Height-width ratio	Lifter height (mm)	Lifter width (mm)	Rotation speed (rad/min)	Number of lifters	Simulation time (s)
5:1	12.5	2.5			
3:1	12	4			
1:1	12	12	6	12	8
1:3	4	12			
1:5	2.5	12.5			

Figure 8 shows that the steel balls were more likely to follow a cataracting motion and collide with the ore particles when the height-width ratio of the lifters was 5:1, 3:1, or 1:1. In the experiments with height-width ratios of 1:3 and 1:5, the lifting effect of the steel balls was poor. The steel balls mainly followed a cascading motion, which does not produce collisions with ore particles. Also, this lifter profile does not provide effective protection to the cylinder due to too much friction between the media and the cylinder.

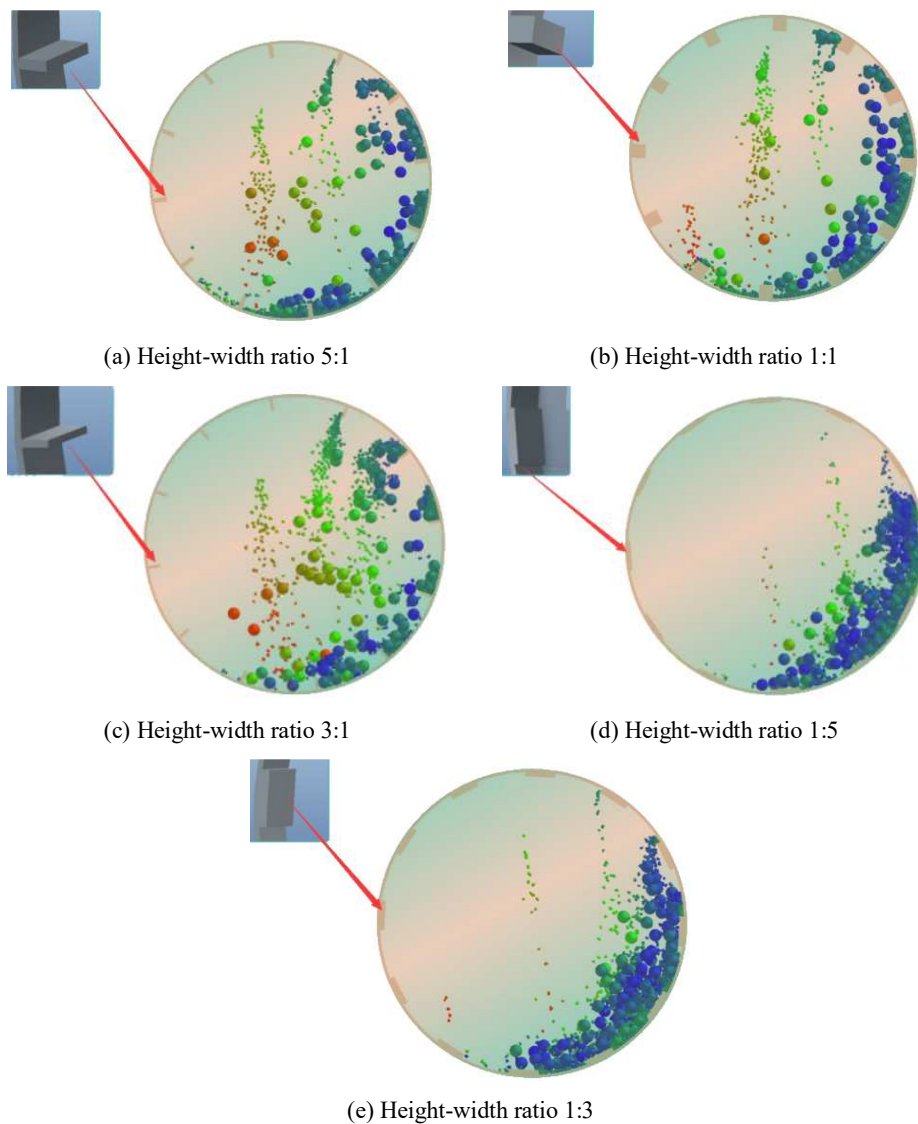


Figure 7 Different height–width ratios of the lifters.

Figure 8 shows a relation graph of the height–width ratio of the rectangular lifters and the milling rate of the ball mill. The height–width of 1:3 is at the lowest point of the curve and then the milling rate of the ball mill begins to rise. When the height–width ratio was 3:1, the maximum milling rate was reached. After that, the milling rate began to decrease with the increase of the aspect ratio. However, the milling rate at a height–width ratio of 5:1 was still higher

than that of the 1:3 and 1:5 height–width ratios. Figure 9 shows the relationship between the number of contacts and the time. When the height–width ratio was 1:3 or 1:5, the number of contacts between all particles was very high, but most of the particles followed a cascading motion and therefore the breakage effect was poor. In contrast, with the remaining three kinds of height–width ratios, the number of contacts between all particles was smaller than 18,000 times, but most of the particles followed a cataracting motion. Therefore, the breakage effect was better.

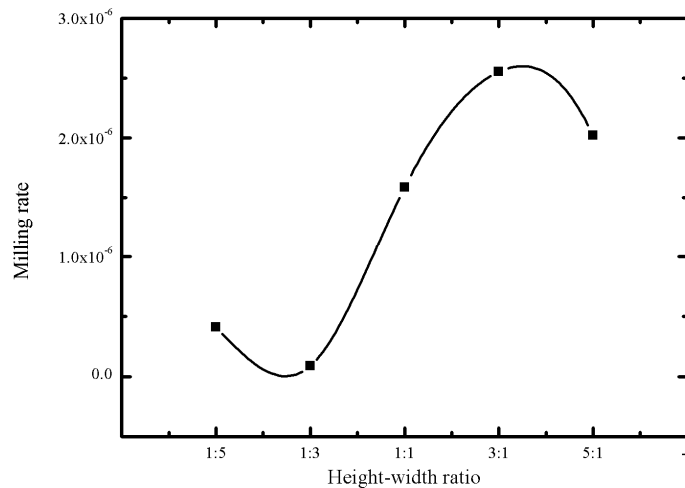


Figure 8 Relationship between milling rate and different lifter height–width ratios.

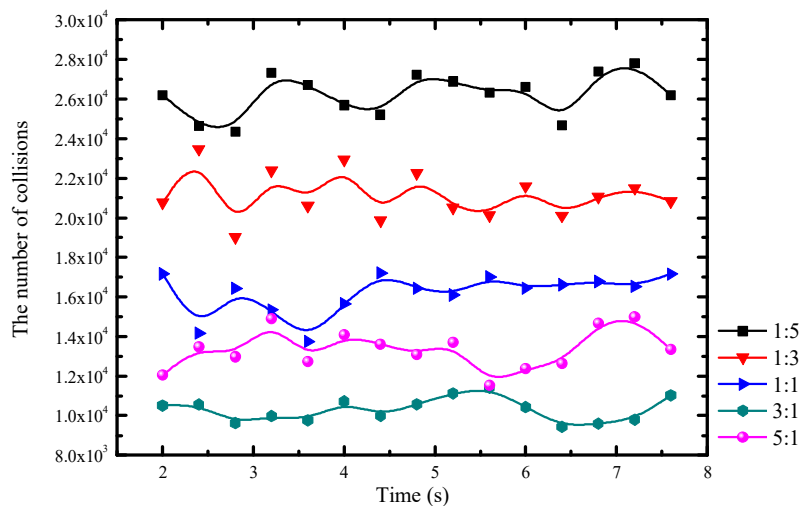


Figure 9 Number of collisions for different lifter height–width ratios.

3.4 Influence of the Rectangular Lifter Height

One of the important parameters in the height-width ratio discussed in the previous section is the height of the rectangular lifters. The height of the rectangular lifters affects the lifting height of the media and the service life of the liner. If the height of the lifters is too high, the amount of medium and ore in the lifting area will be too large, which could make the internal stress of the lifters exceed the stress and breakage limit. In contrast, if the height of the lifters is too short, the lifters are not able to effectively raise the media and the ball mill crushing efficiency will be poor. Hence, the height of the lifters is critical. In this study, four sets of lifters with heights of 5 mm, 12 mm, 15 mm and 18 mm respectively were set up to simulate a reasonable height of the rectangular lifters. The simulation scheme is shown in Table 4.

Table 4 Parameter settings of rectangular lifter height.

Lifter height (mm)	Lifter width (mm)	Rotation speed (rad/min)	Number of lifters	Simulation time (s)
5				
12	4	5	12	10
15				
18				

Figure 10 shows that when the height of the lifters was small, only small particles were raised by the lifters, while large media particles were not raised. Hence, in this situation the breakage effect was poor. When the height of the lifters was increased, large media particles could be raised to a higher position, and were more conducive to the occurrence of a cataracting motion of the particles, resulting in better crushing.

In Figures 11 and 12, it is apparent that the relative lifting height, which is the ratio between the elevated height of the media and the height of the lifters had a significant increasing trend from 5 mm to 12 mm on the height of the lifters. At the same time, the milling rate was significantly improved too. When the height of lifters changed from 12 mm to 18 mm, the relative lifting height was only slightly increased. The maximum milling rate occurred when the height of the lifters was about 13 mm, after which the milling rate would decrease when the height of the lifters was further increased.

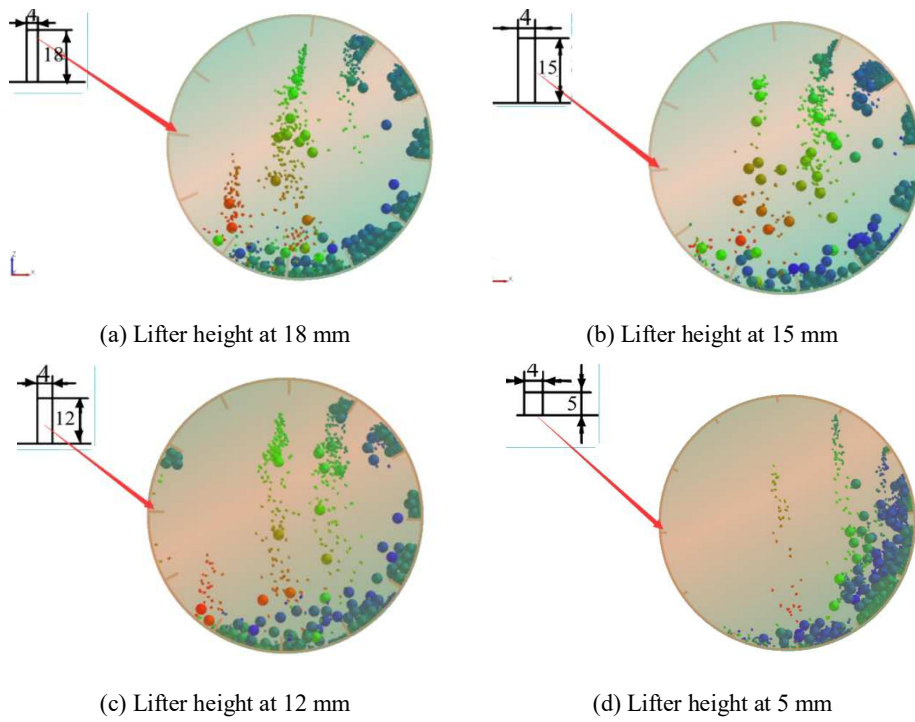


Figure 10 Different lifter heights.

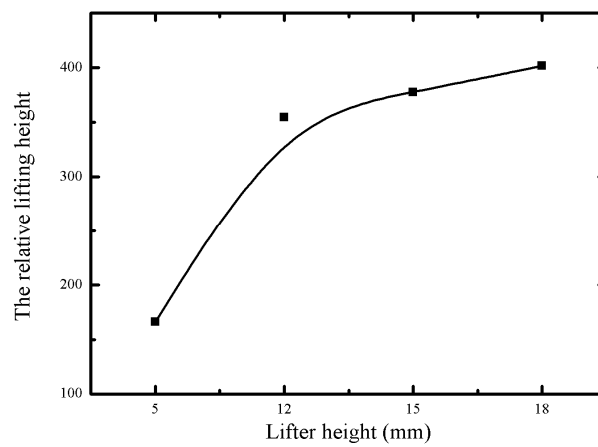


Figure 11 Relationship between relative lifting height and different lifter heights.

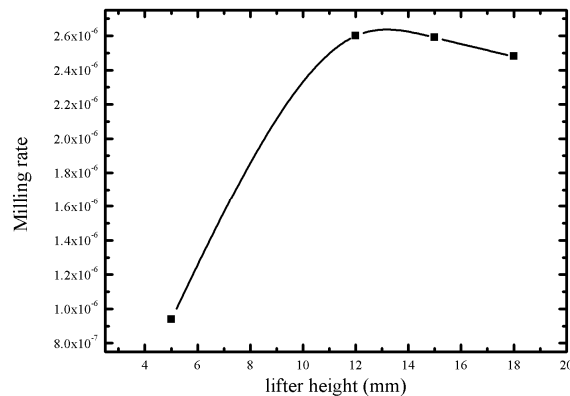


Figure 12 Relationship between milling rate and different lifter heights.

From the above analysis, it can be seen that the increase in height of the lifters affects the relative lifting height of the media and the breakage effect of the ball mill. If the lifters are too high, energy is easily wasted and the lifters easily break. If the lifters are too low, the breakage effect of the ball mill is poor and the lifters cannot protect the cylinder. According to the above simulation results, the height of lifters should be 0.5-1.5 times the diameter of the medium to maximize the breakage effect of the ball mill.

3.5 Influence of the Number of Lifters

The number of lifters influences the trajectory and the lifted height of the media. Industrial experience (Mine Manual Volume) suggests that between 8 and 16 lifters is appropriate. So in this paper, five sets of simulation experiments with 0, 4, 8, 12, and 18 lifters were conducted to study the most appropriate number of lifters. The experimental scheme is shown in Table 5.

Table 5 Parameter settings for number of lifters.

Number of lifters	Lifter height (mm)	Lifter width (mm)	Rotation speed (rad/min)	Simulation time (s)
0				
4				
8	12	4	5	10
12				
18				

When the number of lifters was zero, the media and the ore attached themselves to the wall of the cylinder and followed a cascading motion. Because the media was not raised high enough, the breakage effect of the ore particles was poor. Due to the absence of the lifter's protection, the media and ore directly rubbed against the cylinder wall of the ball mill, resulting in serious damage to the wall.

With an increasing number of lifters, the height of the media also increased so that the breakage effect of the ore was improved. According to Figure 13(e), when there were too many lifters, the collision area of the media and ore decreased. This seriously affects the production efficiency of the ball mill.

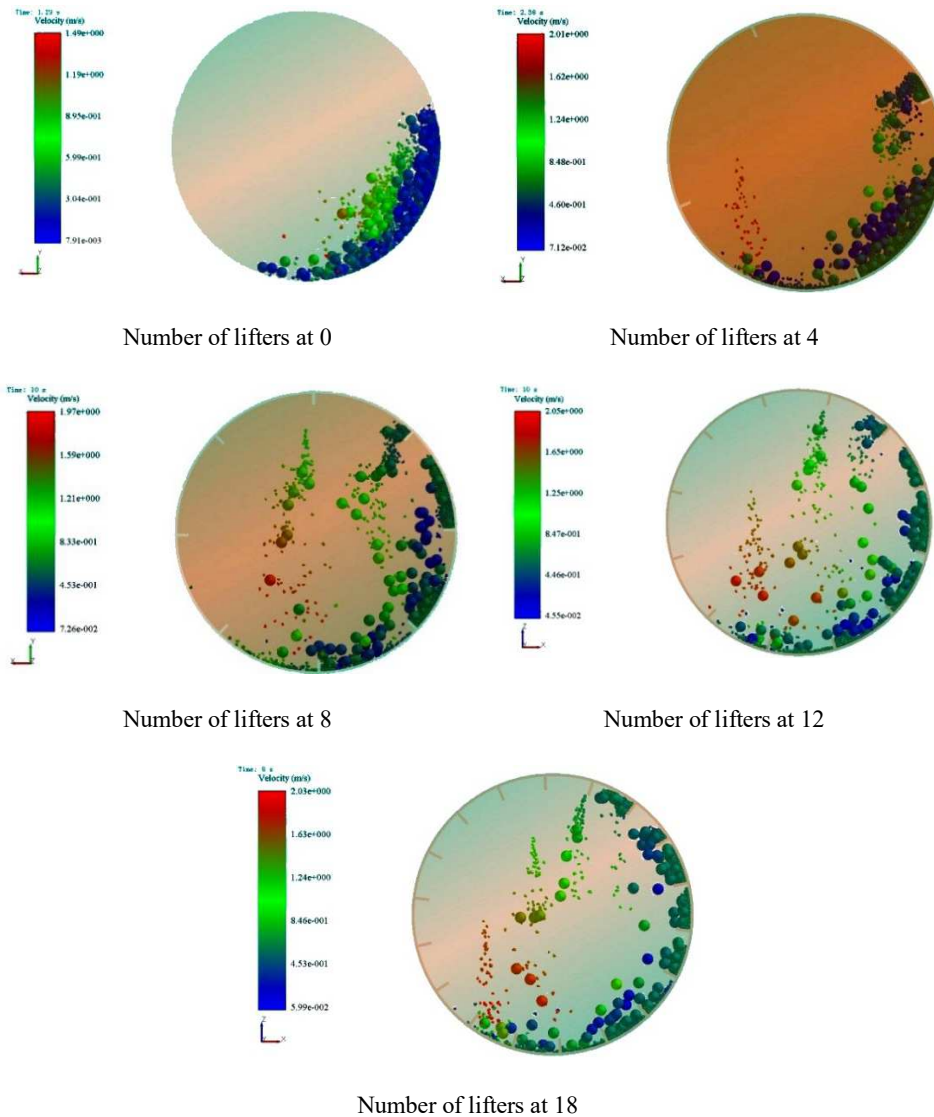


Figure 13 Different numbers of lifters.

As Figure 15 shows, as the number of lifters was increased from 0 to 18, the number of contacts between the particles decreased. Because the particles were separated in several small lattices, the possibility of collisions between the particles was reduced. It can be seen from Figure 14 that the milling rate gradually increased when the number of lifters changed from 0 to 12 and then began to fall. As the number of lifters increased, more and more steel balls were raised to a higher position, impacting the ore particles. But when the number of lifters was too large, the distribution of ore particles was too scattered, which made the possibility smaller of having a collision between the media and the ore particles. In this situation, even if the steel balls have huge kinetic energy, the breakage effect is not very good.

In summary, our analysis can explain that the number of lifters is not necessarily the more the better, because increasing the number of lifters too much reduces the ore crushing efficiency. This is because when the space between the lifters is too tight, the storage capacity between the lifters is reduced and the effective impact of the medium against the ore is reduced and the probability of impact against the lifters is increased, causing the lifters to fail for a long time under the impact of the medium. This should be avoided in actual production. Based on the experimental simulation data results, having twelve lifters in the ball mill produced the best efficiency.

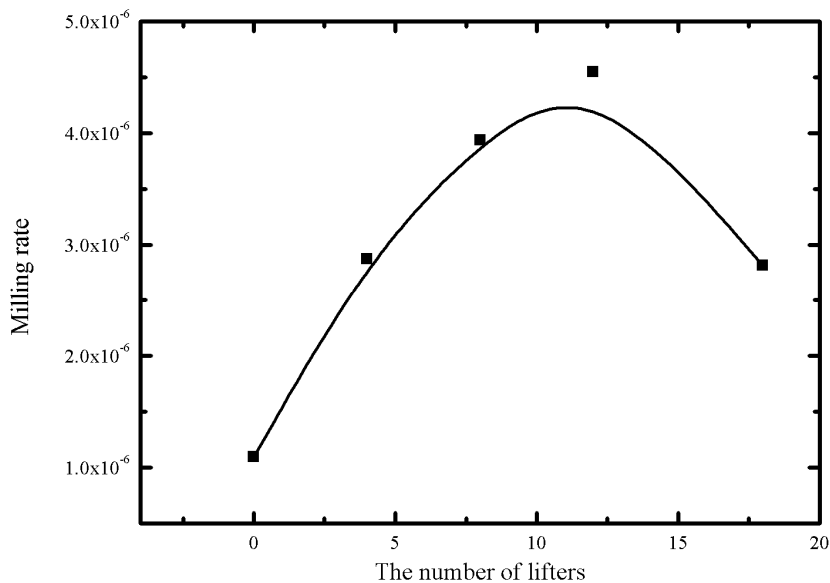


Figure 14 Relationship between milling rate and number of lifters.

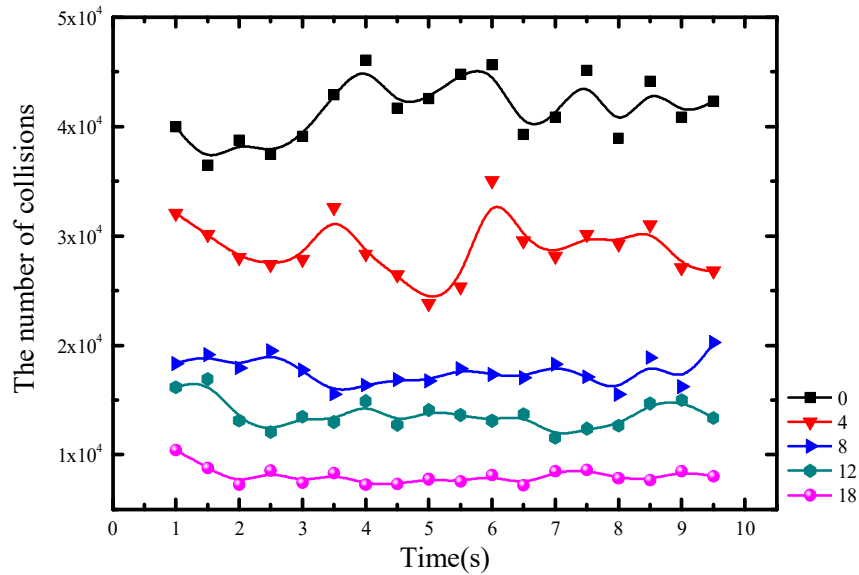


Figure 15 Number of collisions and number of lifters.

4 Coupling Analysis of Mill Lifter Wear

On the one hand, the mill lifters raise the particles, on the other hand, they impact the particles. Deformation and wear of the mill lifters are factors that affect the performance of a ball mill. FEM and DEM were coupled to simulate the interactions between the particles and the mill lifters. It is a feasible way to predict the stress distribution and deformation of the mill lifters. The advantage of DEM is the ability to calculate every particle's motion information (position, pressure and velocity). FEM was employed to analyze the stress distribution on the lifters. In this study, the contact load between the particles, the lifters and the structure was derived from DEM, after which the nodal load was converted to finite element with the relevant positions from DEM. Meanwhile, boundary conditions were defined, including constraints and locations where forces act upon, total deformation, equivalent stress and strain energy are presented and explicated in this section. Without considering the effect on particle motion from the deformation of the equipment, one-way coupling was mainly used in the case of small deformations of the equipment. The definitions of the liner material, density, and Poisson's ratio were set. Considering the mesh number and mesh quality, the grid size was set to 50 mm. The number of grid nodes was 43692, and the number of grid cells was 23635. After meshing, the constraints were added to the FEM model. By solution processing, the corresponding data were obtained.

Figures 16(a), (b), and (c) show the total deformation, equivalent stress and strain energy of the mill lifters predicted over 10 seconds of operation. Figure 16(a) shows the total deformation of rectangular mill liners by optimization in the last section. When particles move steadily in the ball mill, every rectangular lifter bears average pressure, and the displacement and deformation of the mill lifters, caused by the interactions between the particles and the mill lifters, are concentrated in the central position of the plate, so the stress on each plate is higher than average. This indicates that the coupled method (DEM-FEM) contributed to improving the structure by avoiding regional stress concentration. As a major working device, varying the structure of the mill lifters has an effect on efficiency and wear.

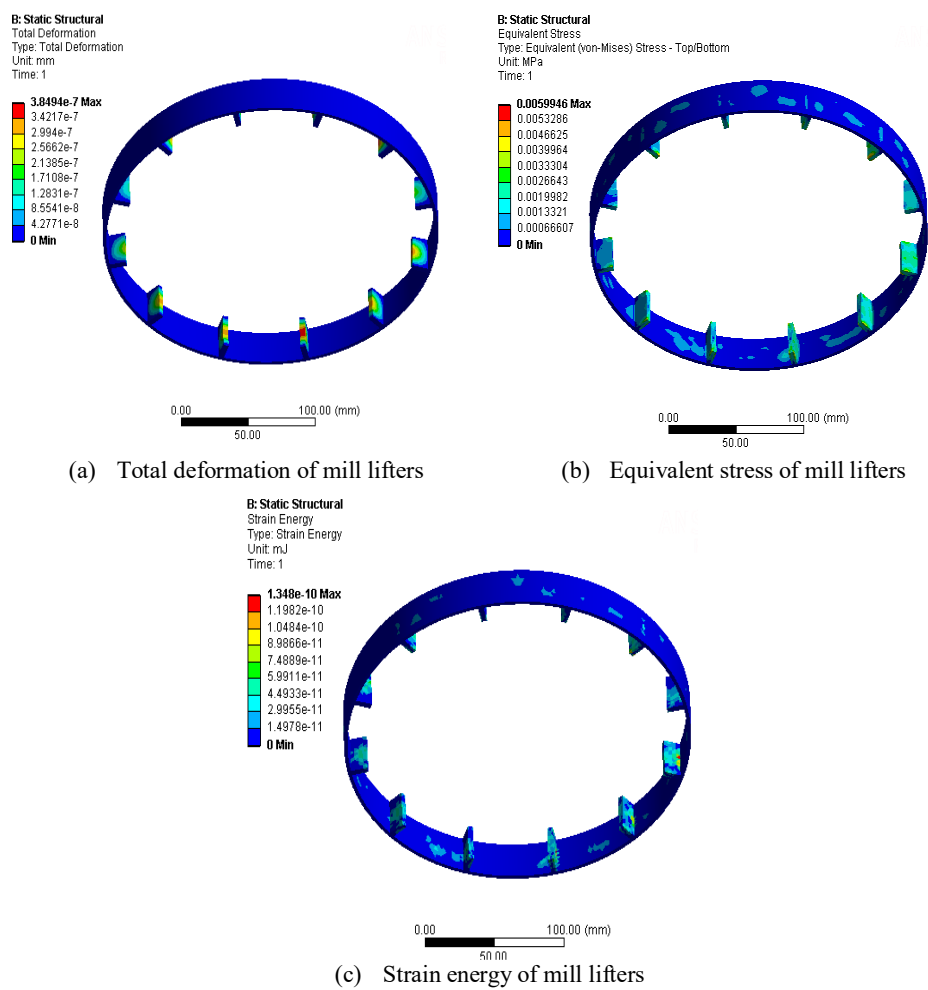


Figure 16 (a), (b), and (c) present the results from DEM-FEM.

Figure 16(b) and Figure 16(c) show the stress and strain energy caused by the particle collisions in the simulated process. Preliminary analysis showed that the maximum values of deformation happen in the middle and upper part of the mill lifters. The stress and strain energy are greater at the bottom of the mill lifters. By not changing them too often, we can improve the structure and surface coating to improve performance. This provides an excellent resolution to multi-objective optimization of ball mills.

5 Conclusion

The profile of the lifters affects the lifting height and trajectory of the particles. Through simulation experiments of five different lifter shapes (rectangular, trapezoidal, triangular, ladder, and semicircle) it was shown that the effect of a rectangular lifter on the lifting of the particles was the best and the milling rate was highest too. Further study on the thickness ratio of the rectangular lifters showed that when the thickness ratio was 3:1, the milling rate of the ball mill was the best.

When the height of the lifters was increased gradually, the lifting height of the media was increased, which enhanced the impact of the media on the ore. When the height of the lifters exceeded 15 mm, the increasing trend of lifting height became less sharp, and the lifters were more likely to break. So a height of the lifters of the 0.5-1.5 times the diameter of media is appropriate. When the number of lifters was less than 12, the milling rate was increased as the number of lifters increased. When the number of lifters was greater than 12, the second-order kinetic energy reduction of the granular system was smaller as the particles collided with the liners and the cylinder, resulting in a decrease in the milling rate of the ball mill. The displacement and deformation of mill lifters caused by the interactions between the particles and the mill lifters was concentrated in the central position of the plates, and the stress on each plate was average. Meanwhile, the stress and strain energy was greater at the bottom of the mill lifters.

Acknowledgements

The authors gratefully acknowledge the support from the Program for Scientific and Technological Innovation Flats of Fujian Province (2014H2002), Fujian Natural Science Foundation (2017J01675), Key Projects of Fujian, Fujian Provincial Youth Natural Fund (JZ160460), and the 51st Scientific Research Fund Program of Fujian University of Technology (GY-Z160139).

References

- [1] Prasher, C., *Crushing and Grinding Process Handbook*, Wiley, Chichester, 1987.
- [2] Mishra, B.K. & Rajamani, R.K., *The Discrete Element Method for the Simulation of Ball Mills*, Application Math Modeling, **16**(16), pp. 598-602, 1992.
- [3] Sinnott, M.D. & Cleary, P. W., *Simulation of Particle Flows and Breakage in Crushers using DEM: Part 1 Compression Crushers*, Minerals Engineering, **74**, pp. 178-197, 2015.
- [4] Garboczi, E.J., Riding, K.A. & Mohammadreza, M., *Particle Shape Effects on Particle Size Measurement for Crushed Waste Glass*, Advanced Powder Technology, **28**(2), pp. 648-657, 2017.
- [5] Sinnott, M.D., Cleary, P.W. & Morrison, R.D., *Combined DEM and SPH Simulation of Overflow Ball Mill Discharge and Trommel Flow*, Minerals Engineering, **108**, pp. 93-108, 2017.
- [6] Sinnott, M.D. & Cleary, P.W., *Simulation of Particle Flows and Breakage in Crushers using DEM: Part 2 – Impact Crushers*, Minerals Engineering, **74**, pp. 163-177, 2015
- [7] Cleary, P.W. & Morrison, R.D. *Understanding Fine Ore Breakage in Laboratory Scale Ball Mill using DEM*, Minerals Engineering, **24**, pp. 352-366, 2011.
- [8] Cleary, P.W., Sinnott, M.D., Morrison, R.D. & Cummins, G.W., *Delaney Analysis of Cone Crusher Performance with Changes in Material Properties and Operating Conditions using DEM*, Mineral Engineering, **100**, pp. 49-70, 2017.
- [9] Yasuhiro, Y., Rikio, S., Junya, K. & Fumio, S., *DEM Simulation of Bead Motion During Wet Bead Milling using an Enlarged Particle Model*, International Journal of Mineral Processing, **114**(117), pp. 93-99, 2012.
- [10] Djordjevic, N., *Influence of Charge Size Distribution on net Power Draw of Tumbling Mill Based on DEM Modeling*, Minerals Engineering, **18**, pp. 375-378, 2005
- [11] Djordjevic, N., *Discrete Element Modelling of the Influence of Lifters on Power Draw of Tumbling Mills*, Minerals Engineering, **16**(4), pp. 331-336, 2003.
- [12] Wang, M.H., Yang, R.Y. & Yu, A.B., *DEM Investigation of Energy Distribution and Particle Breakage in Tumbling Ball Mills*, Powder Technology, **223**(6), pp. 83-91, 2012.
- [13] Bracey, R.J., Weerasekara, N.S. & Powell, M.S., *Performance Evaluation of the Novel Multi-shaft Mill using DEM*, Minerals Engineering, **98**, pp. 251-260, 2016.
- [14] Bian, X., Wang, G., Wang, H., Wang, S. & Lu, W., *Effect of Lifters and Mill Speed on Particle Behavior, Torque, and Power Consumption of a*

- Tumbling Ball Mill: Experimental Study and DEM Simulation*, Minerals Engineering, **105**, pp. 22-35, 2017.
- [15] Yu, P., Xie, W.G., Liu, L.X. & Powell, M.S., *Analytical Solution for the Dynamic Model of Tumbling Mills*, Powder Technology, In Press, Corrected Proof, <https://doi.org/10.1016/j.powtec.2017.04.035>, 2017.
- [16] Carvalho, Rodrigo M. de & Tavares, Luís Marcelo, *Predicting the Effect of Operating and Design Variables on Breakage Rates using the Mechanistic Ball Mill Model*, Minerals Engineering, **43-44**, pp. 91-101, 2013.
- [17] Cleary, P.W., *Large Scale Industrial DEM Modeling*, Engineering Computations, **21**(2), pp. 169-204. 2004.
- [18] Cleary, P.W., *DEM Prediction of Industrial and Geophysical Particle Flows*, Particuology, **8**(2), pp. 106-118. 2010.
- [19] Li, Z., Tong, X., Zhou, B. & Wang, X., *Modeling and Parameter Optimization for the Design of Vibrating Screens*, Minerals Engineering, **83**, pp. 149-155, 2015.
- [20] Li, Z., Tong, X., Xia, H. & Yu, L., *A Study of Particles Looseness in Screening Process of a Linear Vibrating Screen*, Journal of Vibroengineering, **18**(2), pp. 671-681, 2016.
- [21] Li, Z.F. & Tong, X., *Applications of the Discrete Element Method and Fibonacci Sequence on a Banana Screen*, Journal of Engineering, Design and Technology, **15**(1), pp. 2-12, 2017
- [22] Wang, W., Liu, Y., Zhu, G. & Liu, K., *Using FEM-DEM Coupling Method to Study Three-body Friction Behavior*, Wear, **318**(2), pp. 114-123, 2014.
- [23] Murugaratnam, K., Utili, S. & Petrinic, N., *A Combined DEM-FEM Numerical Method for Shot Peening Parameter Optimisation*, Advances in Engineering Software, **79**(C), pp. 13-26, 2015.
- [24] Xia, H., Tong, X., Li, Z. & Wu, X., *DEM-FEM Coupling Simulations of the Interactions between Particles and Screen Surface of Vibrating Screen*, Int. J. Mining and Mineral Engineering, **8**(3), pp. 250-263, 2017.
- [25] Jonsén, P., Palsson, B.I. & Tano, K., *Prediction of Mill Structure Behaviour in a Tumbling Mill*, Minerals Engineering, **24**(3), pp. 236-244, 2011.
- [26] Cundall, P.A. & Strack, O.D.L., *A Discrete Numerical Model for Granular Assemblies*, Geotechnique, **30**(30), pp. 331-336, 1979.